Title: **An Analysis Code and a Planning Tool Based on a Key Element Index for Controlled Explosive Demolition**

Author: Daigoro Isobe, Division of Engineering Mechanics and Energy, University of Tsukuba

Subjects:

Keywords: Building Code
Demolition

Publication Date: 2014

Original Publication: International Journal of High-Rise Buildings Volume 3 Number 4

Paper Type:
1. Book chapter/Part chapter
2. **Journal paper**
3. Conference proceeding
4. Unpublished conference paper
5. Magazine article
6. Unpublished

International Journal of High-Rise Buildings
December 2014, Vol 3, No 4, 243-254

International Journal of
High-Rise Buildings
www.ctbuh-korea.org/ijhrb/index.php

An Analysis Code and a Planning Tool Based on a Key Element Index for Controlled Explosive Demolition

Daigoro Isobe†

Division of Engineering Mechanics and Energy, University of Tsukuba, Ibaraki 305-8573, Japan

Abstract

In this study, a demolition analysis code using the adaptively shifted integration (ASI)-Gauss technique, which describes structural member fracture by shifting the numerical integration point to an appropriate position and simultaneously releasing the sectional forces in the element, is developed. The code was verified and validated by comparing the predicted results with those of several experiments. A demolition planning tool utilizing the concept of a key element index, which explicitly indicates the contribution of each structural column to the vertical load capacity of the structure, is also develped. Two methods of selecting specific columns to efficiently demolish the whole structure are demonstrated: selecting the columns from the largest index value and from the smallest index value. The demolition results are confirmed numerically by conducting collapse analyses using the ASI-Gauss technique. The numerical results suggest that to achieve a successful demolition, a group of columns with the largest key element index values should be selected when explosives are ignited in a simultaneous blast, whereas those with the smallest should be selected when explosives are ignited in a sequence, with a final blast set on a column with large index value.

Keywords: Controlled explosive demolition, Key element index, Collapse analysis, Finite element method, ASI-Gauss technique

1. Introduction

The technology used in the demolition of old or uninhabitable buildings has always been of major interest in civil engineering and remains a challenge in engineering practice. Because conventional demolition techniques that use a hydraulic concrete crusher, a concrete cutter or a nonexplosive demolition agent are lengthy and costly, demolition techniques using controlled explosives are often used to meet the heavy demand for demolition work. Although this method increases work efficiency, it also poses a high risk of damage to neighboring buildings, especially in urban areas [1]. Furthermore, explosive demolition requires high levels of knowledge and experience [2,3], which are very difficult for general engineers to master. Although there are several explosive demolition companies currently working in the USA and Europe, the demolition technique has been only used in a few cases in Japan, which may or may not be due to the above reasons. To help familiarize Japanese construction companies with explosive demolition methods, numerical assumptions using computational analysis will be essential in ensuring the success of this technique.

To date, only a few numerical codes have shown high performance when modeling structurally discontinuous problems; e.g., the distinct element method (DEM) [4] and discontinuous deformation analysis (DDA) [5] have been successfully applied to model overall collapse phenomena [6-9]. The Applied Element Method (AEM) [10], which can predict crack initiation and propagation in the material and can also follow the total behavior from zero loading to complete collapse, has also been applied to blast demolition analysis of structures. However, the above-mentioned discrete numerical methods need many assumptions on the models with less physical meanings, and there are still no adequate numerical procedures available to accurately track the explosive demolition process, which includes coupled and complicated failure mechanisms of structural frame members.

The first objective of this study was to develop an analysis code for explosive demolition that can explicitly express member fracture and elemental contact in the demolition process. This code is based on the adaptively shifted integration (ASI)-Gauss technique [11], which is a modified version of the previously developed ASI technique [12,13] for the linear Timoshenko beam element and computes highly accurate elastoplastic solutions even with the minimum number of elements per member. The ASI-Gauss technique obtains an even higher accuracy, particularly in the elastic range, by placing the numerical integration points of the two consecutive elements to form an elastically deformed member so that stresses and strains are evaluated at the Gaussian integration points of the two-element member. Moreover, the technique can be

†Corresponding author: Daigoro Isobe
Tel: +81-29-853-6191; Fax: +81-29-853-5207
E-mail: isobe@kz.tsukuba.ac.jp

used to express member fracture by shifting the numerical integration point to an appropriate position and simultaneously releasing the sectional forces in the element. The numerical code was validated herein by comparing the numerical results with a simple impact test and a simulated demolition experiment.

The second objective of this study was to develop a demolition planning tool based on a parameter called the key element index, which indicates the contribution of a structural column to the vertical capacity of the structure. Two ways of selecting specific columns to demolish the whole structure are demonstrated: selecting the columns from the largest index value and from the smallest index value. The demolition results are confirmed numerically by carrying out collapse analyses using the ASI-Gauss technique, and the tendencies of the demolition modes to follow the key element index values are estimated.

This paper is organized as follows. Section 2 introduces the outline of the ASI-Gauss technique and the member-fracture and elemental-contact algorithms. In Section 3, several examples are presented for the validation of the numerical code. Section 4 presents the concept of the key element index and the demolition planning tool developed using the index values, followed by numerical examples. Finally, Section 5 concludes the paper.

2. Numerical Methods for Collapse Analysis

The general concepts of the ASI-Gauss technique are explained in this section. The algorithms concerning member fracture and elemental contact are then described.

2.1. The ASI-Gauss technique

Fig. 1 shows a linear Timoshenko beam element and its physical equivalence to the rigid body-spring model (RBSM). As shown in the figure, the relationship between the locations of the numerical integration point and the stress evaluation point where a plastic hinge is actually formed is expressed as [14]

$$r = -s \tag{1}$$

In the above equation, s is the location of the numerical integration point, and r is the location where stresses and strains are actually evaluated. We refer to r as the stress evaluation point hereinafter. The variables s and r are dimensionless quantities that take values between -1 and 1.

In both the ASI and ASI-Gauss techniques, the numerical integration point is shifted adaptively to form a plastic hinge at exactly the point where a fully plastic section is formed. When the plastic hinge is determined to be unloaded, the corresponding numerical integration point is shifted back to its normal position. Here, the normal position indicates the location where the numerical integration point is placed when the element acts elastically. By doing so, the plastic behavior of the element is simulated

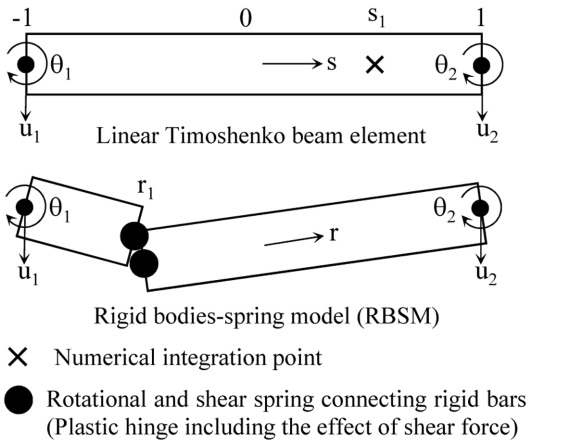

Figure 1. Linear Timoshenko beam element and its physical equivalent.

appropriately, and a convergent solution is achieved with only a small number of elements per member. However, in the ASI technique, the numerical integration point is placed at the midpoint of the linear Timoshenko beam element, which is considered to be optimal for one-point integration, when the entire region of the element behaves elastically. When the number of elements per member is very small, solutions in the elastic range are inaccurate because one-point integration is used to evaluate the low-order displacement function of the beam element.

The main difference between the ASI and ASI-Gauss techniques lies in the location of the normal position of the numerical integration point. In the ASI-Gauss technique, two consecutive elements that form a member are considered as a subset, and the numerical integration points of an elastically deformed member are placed so that the stress evaluation points coincide with the Gaussian integration points of the member. This placement means that stresses and strains are evaluated at the Gaussian integration points of elastically deformed members. Gaussian integration points are optimal for two-point integration, and the accuracy of bending deformation is mathematically guaranteed [15]. In this way, the ASI-Gauss technique has the advantages of two-point integration while using one-point integration in the actual calculations.

Fig. 2 shows the differing locations of the numerical integration points of elastically deformed elements in the ASI and ASI-Gauss techniques. The elemental stiffness matrix, generalized strain and sectional force increment vectors in the elastic range for the ASI technique are given by Eqs. (2), and those for the ASI-Gauss technique are given by Eqs. (3).

$$[K] = L[B(0)]^T[D(0)][B(0)] \tag{2a}$$

$$\{\Delta\varepsilon(0)\} = [B(0)]\{\Delta u\} \tag{2b}$$

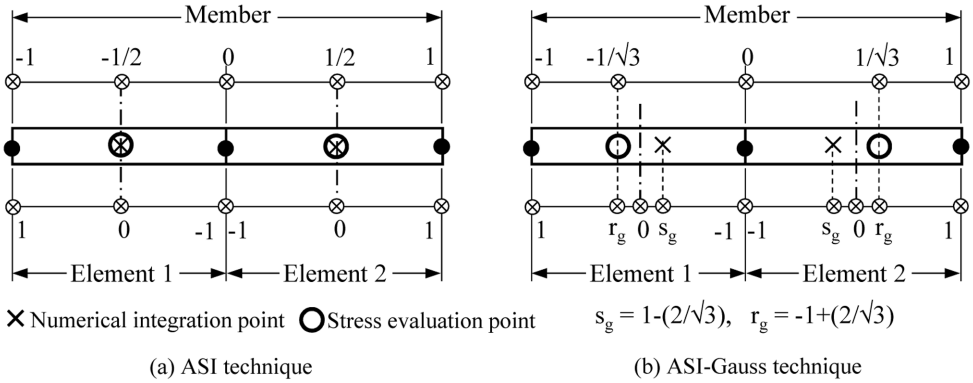

Figure 2. Locations of the numerical integration and stress evaluation points in the elastic range.

$$\{\Delta\sigma(0)\}=[D(0)]\{\Delta\varepsilon(0)\} \tag{2c}$$

$$[K]=L[B(s_g)]^T[D(r_g)][B(s_g)] \tag{3a}$$

$$\{\Delta\varepsilon(r_g)\}=[B(s_g)]\{\Delta u\} \tag{3b}$$

$$\{\Delta\sigma(r_g)\}=[D(r_g)]\{\Delta\varepsilon(r_g)\} \tag{3c}$$

$$s_g=1-\frac{2}{\sqrt{3}},\quad r_g=-1+\frac{2}{\sqrt{3}} \tag{3d}$$

Here, $\{\Delta\varepsilon\}$, $\{\Delta\sigma\}$ and $\{\Delta u\}$ are the generalized strain increment vector, generalized stress (sectional force) increment vector and nodal displacement increment vector, respectively. $[B]$ is the generalized strain-nodal displacement matrix, $[D]$ is the stress-strain matrix and L is the length of the element.

The plastic potential used in this study is expressed by:

$$f\equiv\left(\frac{M_x}{M_{x0}}\right)^2+\left(\frac{M_y}{M_{y0}}\right)^2+\left(\frac{N}{N_0}\right)^2-1=f_y-1=0 \tag{4}$$

Here, f_y is the yield function, and M_x , M_y and N are the bending moments around the x- and y-axes and the axial force, respectively. The terms with the subscript 0 are the values that result in a fully plastic section in an element when acting independently on a cross-section. The validity of the ASI-Gauss technique in elastoplastic analyses under static and dynamic loadings were confirmed by various numerical tests [11].

2.2. Member fracture algorithm

Fig. 3 shows the locations of the numerical integration points for each stage in the ASI-Gauss technique. A plastic hinge is normally generated before it develops into a member fracture, and the formation of a plastic hinge is described by shifting the numerical integration point to the opposite end of the fully plastic section according to Eq. (1). For example, if a fully plastic section first occurs at the right end of an element ($r = 1$) as shown in the figure, the numerical integration point is immediately shifted to the left end of the element ($s = -1$). Simultaneously, the numerical integration point of the adjacent element forming the same member is shifted back to its midpoint, the location appropriate for one-point integration. Member fracture is expressed by reducing the sectional forces of the element immediately after the occurrence of a fractured section on either end of the element. The released force vector $\{F\}$, which operates on the element at the next step if a fractured section first occurs at the right end

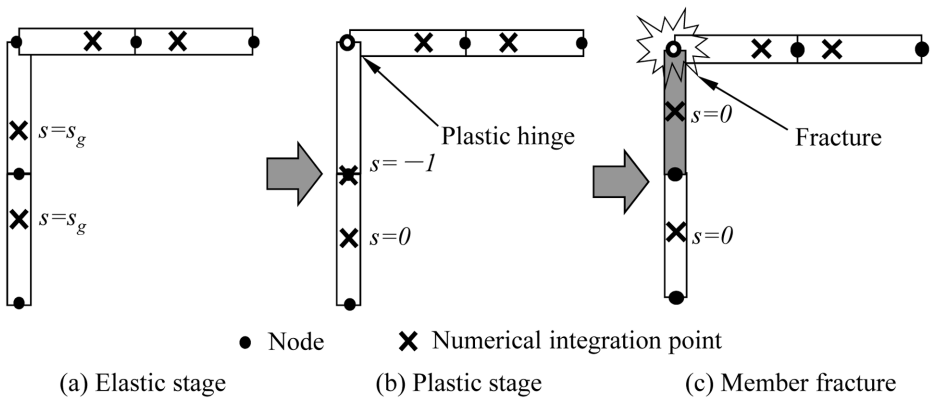

Figure 3. Locations of the numerical integration points for each stage in the ASI-Gauss technique.

of an element ($r = 1$), is expressed by the following equation:

$$\{F\} = L[B(-1)]^T \{\sigma(1)\} \tag{5}$$

Similarly, if a fully plastic section or a fractured section first occurs at the left end of the element ($r = -1$), the numerical integration point is shifted to the right end of the element ($s = 1$).

In this study, member fracture is determined using bending strains, shear strains and axial tensile strains that occur in the elements, as shown in the following equation:

$$\left|\frac{\kappa_x}{\kappa_{x0}}\right| - 1 \geq 0 \quad \text{or} \quad \left|\frac{\kappa_y}{\kappa_{y0}}\right| - 1 \geq 0 \quad \text{or} \quad \left|\frac{\gamma_{xz}}{\gamma_{xz0}}\right| - 1 \geq 0 \quad \text{or} \tag{6}$$

$$\left|\frac{\gamma_{yz}}{\gamma_{yz0}}\right| - 1 \geq 0 \quad \text{or} \quad \left(\frac{\varepsilon_z}{\varepsilon_{z0}}\right) - 1 \geq 0$$

where κ_x, κ_y, γ_{xz}, γ_{yz}, ε_z, κ_{x0}, κ_{y0}, γ_{xz0}, γ_{yz0} and ε_{z0} are the bending strains around the x- and y-axes, the shear strains for the x- and y-axes, the axial tensile strain and the critical values for these strains, respectively. The critical strain values used in the analysis were obtained from laboratory experiments using high strength joint bolts [16].

2.3. Elemental contact algorithm

A set of two elements in potential contact is first selected by evaluating the shortest distance between them using the geometric relations of the four nodes (see Fig. 4(a)). By examining the angles between the assumed contact point M and two nodes, a final determination of contact is made if the angles $\angle MB_1B_2$ and $\angle MB_2B_1$ are both acute (see Fig. 4(b)); the two elements will not come in contact if one of the angles is obtuse (see Fig. 4(c)). Once they are determined to be in contact, the elements are bound with a total of four gap elements between the nodes (see Fig. 4(d)). The sectional forces are delivered through these gap elements to the connecting elements. To express contact release, the gap elements are automatically eliminated at the time when the mean value of the deformation of gap elements is reduced to a specified ratio.

3. Validation of the Methods

To validate the numerical code, we performed a simple impact test with two beams. As shown in Fig. 5, one of the two aluminum beams was rigidly clamped at the both ends, whereas the other was silently dropped with an initial velocity of 0 m/s from the height of 400 mm above the clamped beam. The planned contact point between the two beams is indicated in the figure. The impact and contact phenomenon were observed using a high-speed camera, as shown in Fig. 6(a), and the numerical results obtained using the code based on the ASI-Gauss technique are shown in Fig. 6(b). The two results agree very well, indicating that the contact algorithm implemented in the numerical code performed as intended to model the impact, contact and bounce phenomena.

Next, the code was validated by comparing the obtained results with an experiment performed in the laboratory using an electromagnetic system to experimentally simulate the explosive demolition of a structure [17]. The main features of the experimental system are as follows: two electromagnetic devices (KANETEC, KE-4RA, max. attach force = 110 N, for beams; KE-4B, max. attach force = 400 N, for columns) are mounted on both sides of an aluminum pipe, as shown in Fig. 7, and the members are joined with steel connectors held by the magnetic field generated by the electromagnetic devices. Power is supplied to these devices through a 4-pin connector jack and a telephone cord. The blast intervals and switching of the magnetic field are controlled by the blast interval con-

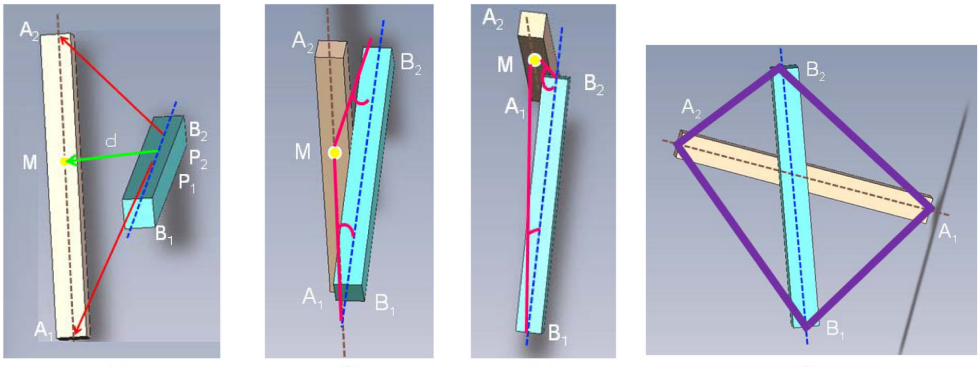

(a) Searching for shortest distance
(b) Contact if both angles are acute
(c) Pass by if one of both angles is obtuse
(d) Gap elements connecting two elements in contact

Figure 4. Elemental contact algorithm.

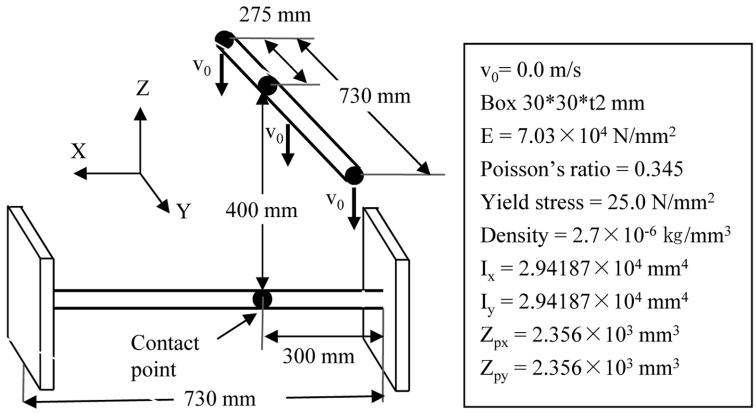

Figure 5. Experimental and analytical conditions for the impact test with two aluminum beams.

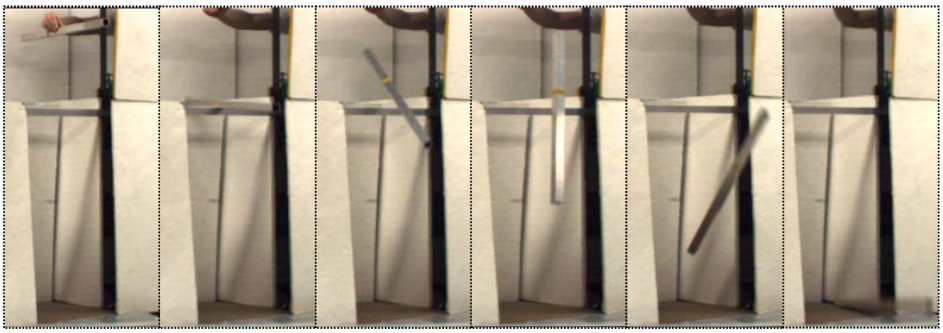

(a) Experimental result

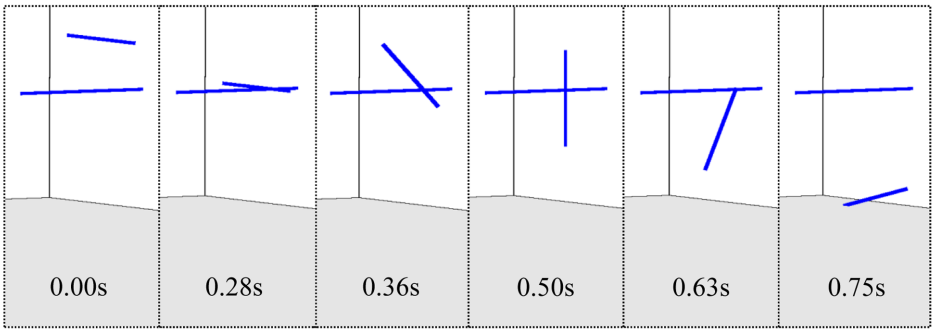

(b) Numerical result

Figure 6. Experimental and numerical results for impact and contact phenomena with two aluminum beams.

troller and power switches, which are connected to a PC and a power supply. The magnetic fields of the devices at each blast point are sequentially released by the PC to simulate member fracture caused by an explosion. The system can simulate the failure of beams by disconnecting the magnetic force between the beams and the columns. However, the column failure cannot be initiated in the electromagnetic system as in the real conditions. The failure of the columns are simulated, first by switching off the electromagnetic field of the column member joints and then, by composing a cantilever system with the upper beam. The purpose of this system is to pile up the demolition test results, easily and safely, to validate the proposed numerical code.

The properties and conditions used for the experiment and the analysis are as follows: each span length was 34 cm (for the beams) or 28 cm (for the columns), with 3 cm × 3 cm box-type beams and 4 cm × 4 cm box-type columns, each with a Young's modulus of 70 GPa and a Poisson ratio of 0.345 (aluminum); the critical values of the bending strains were 2.4×10^{-4} rad/mm (beams) and 3.1×10^{-4} rad/mm (columns); and the tension strains were 2.7×

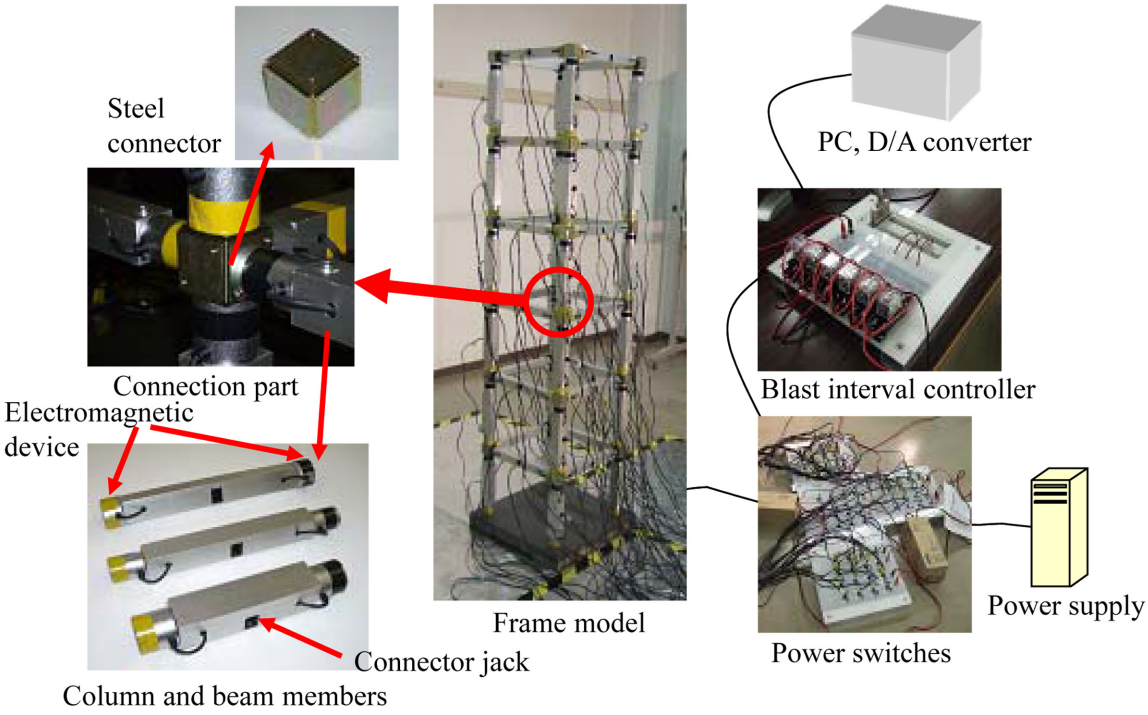

Figure 7. Outline of the simulated blast demolition experimental system.

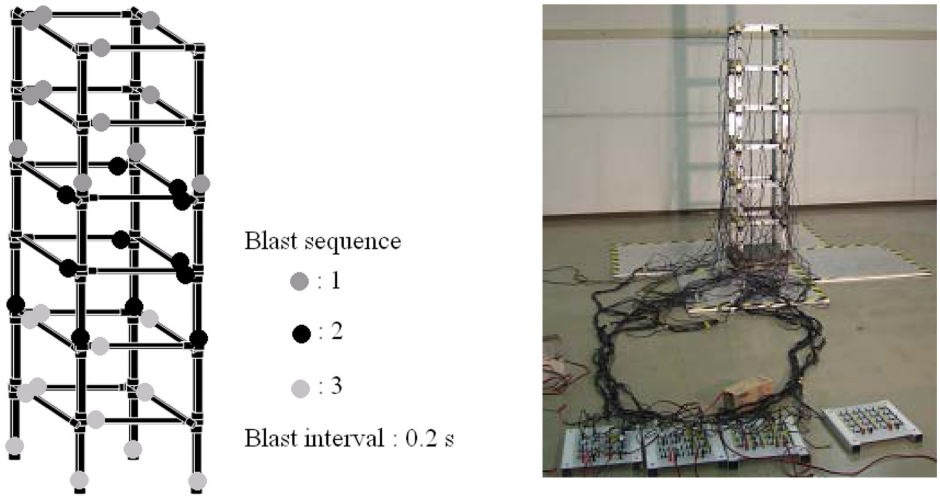

(a) Blast conditions

(b) Experimental setup

Figure 8. Blast conditions for a six-story frame model.

10^{-4} (beams) and 3.0×10^{-4} (columns). A time increment of 0.1 ms was used for the analysis. Numerical damping was applied, however, structural damping was not considered. A six-story frame model was constructed using the described devices. The blast conditions are shown in Fig. 8; the blast points and the blast sequence were carefully selected to enable the floor sections to fold in sequentially starting at the upper floors so as to avoid the dispersal of fragments over a wide area. Fig. 9 shows a comparison of the experimental demolition modes and the numerical results. The expected demolition mode was observed in both cases, and the results are in very good agreement.

4. Blast Demolition Planning Tool using the Key Element Index

In this section, a blast demolition planning tool using the concept of a key element index is first described. Sev-

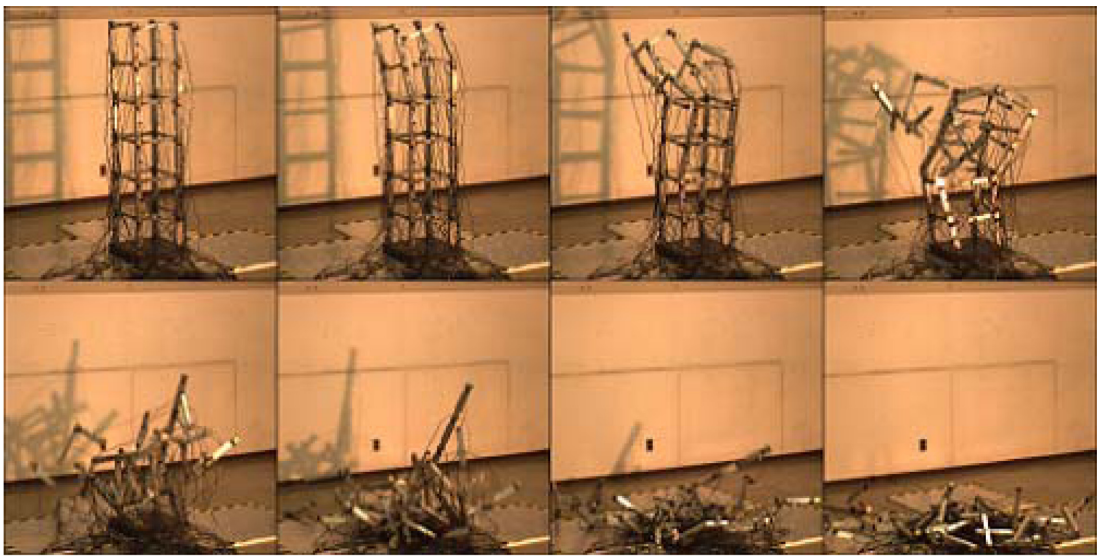

(a) Experimental result

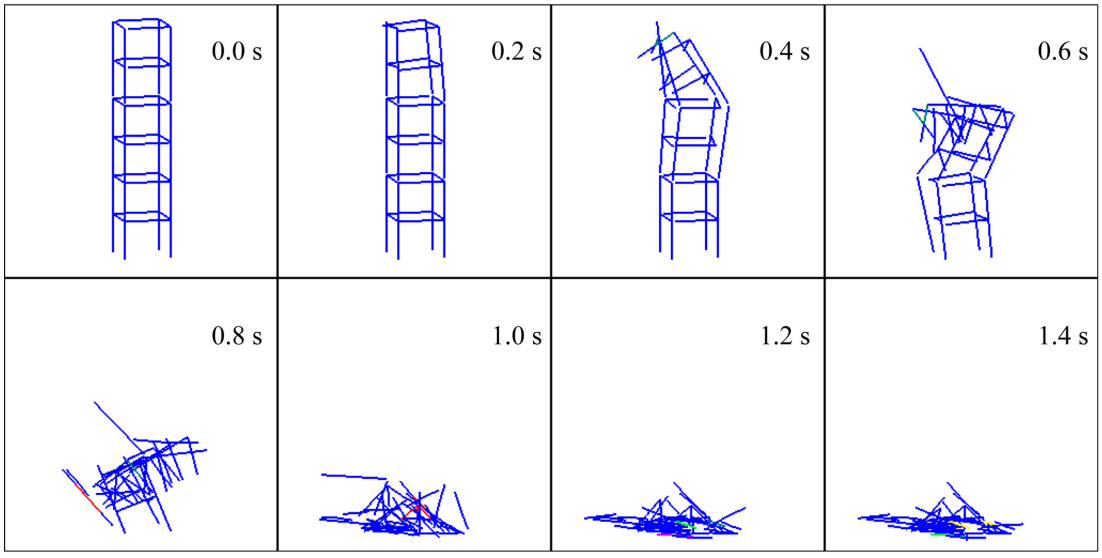

(b) Numerical result

Figure 9. Comparison of demolition modes.

eral numerical analyses are then performed on a 15-story, three-span framed structure using the demolition plans obtained with the planning tool to demonstrate its utility.

4.1. Key element index

Due to variations in their span lengths and strengths, certain columns in a structure support more vertical loads than other columns and thus act as "key elements" in the structure. Several indexes have been developed to evaluate the contribution of each column to the strength of a structure, i.e., to determine the key elements, such as the redundancy index by Frangopol [18] and the sensitivity index by Ito et al. [19]. These indexes are effective for identifying highly sensitive columns that support the vertical load; however, they equivalently identify those columns that only cause partial collapse and are thus not useful for demolition planning, where the major aim is the total collapse of a structure. Therefore, a new index called the key element index for estimating the contribution of base columns to the total collapse of the structure is proposed.

The key element index is calculated as follows. First, we perform a static pushdown analysis by equally applying incremental vertical loads at every structural joint in a modeled structure. Several columns on the upper floors may yield in this process, but the vertical loads are nevertheless continuously applied in steps until one of the base columns yields. The total vertical load (including the

floor loads) applied to a column at the step when one of the base columns yields is defined as the ultimate yield strength P_G of the structure. The ultimate yield strength of the initial, undamaged structure is denoted ${}_0P_G$, and the ultimate yield strength of a structure with one base column eliminated is denoted ${}_1P_G$. The key element index KI of column m, for example, can be defined as the ratio of the ultimate yield strengths of the present and the initial step. The index can thus be written as:

$$ {}^0_1KI_m = {}_0P_G / {}_1P_G \tag{7}$$

The key element index at the nth step is then:

$$ {}^0_nKI_m = {}_0P_G / {}_nP_G \tag{8}$$

The index shown above indicates the contribution of the present column (or columns) to the strength of the initial, undamaged structure and can be used for cases in which the columns are eliminated simultaneously. However, the sensitivity of columns may change momentarily for those cases when the columns are eliminated sequentially within a certain interval. Therefore, the updated index, as shown below, is used for those cases with a sequential blast.

$$ {}^{n-1}_nKI_m = {}_{n-1}P_G / {}_nP_G \tag{9}$$

In this case, the index can be defined as the ratio of the ultimate yield strengths of the present and the previous step.

As an example, the key element index values were calculated for a 15-story, three-span model, as shown in Fig. 10. Each span length is 6 m, and the height between each floor is 3.6 m. The material used for the columns and beams is SN490B steel. We selected box-type section of 430 mm × 430 mm × 13 mm × 13 mm on the 1st floor columns and H-type section of 331 mm × 825.7 mm × 18.4 mm × 13.2 mm for the beams, with the sectional sizes becoming gradually thinner in the higher stories. The floor load, in this case, is set to 400 kgf/m^2. The updated index values and the selection of columns from the largest index value at each step are shown in Fig. 11. For example, the key element index value KI for column No. 16 (in the upper right corner) can be calculated at the first step as:

$$ {}^0_1KI_{16} = {}_0P_G / {}_1P_G = 1.693 \tag{10}$$

and at the second step as:

$$ {}^1_2KI_{16} = {}_1P_G / {}_2P_G = 1.012 \tag{11}$$

In this paper, the column at the left and lower side is selected prior to the other columns, if the index values calculated for multiple columns are the same, to direct the whole collapsing building toward the lower left side. As shown in the figure, the selected columns tend to bias to

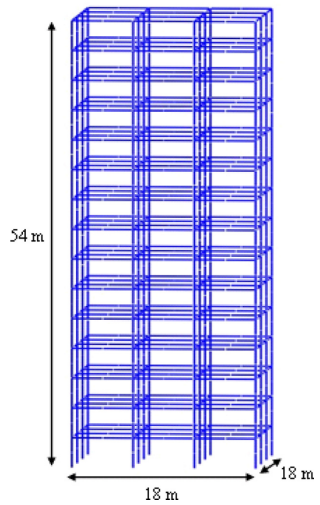

Figure 10. A 15-story, three-span model.

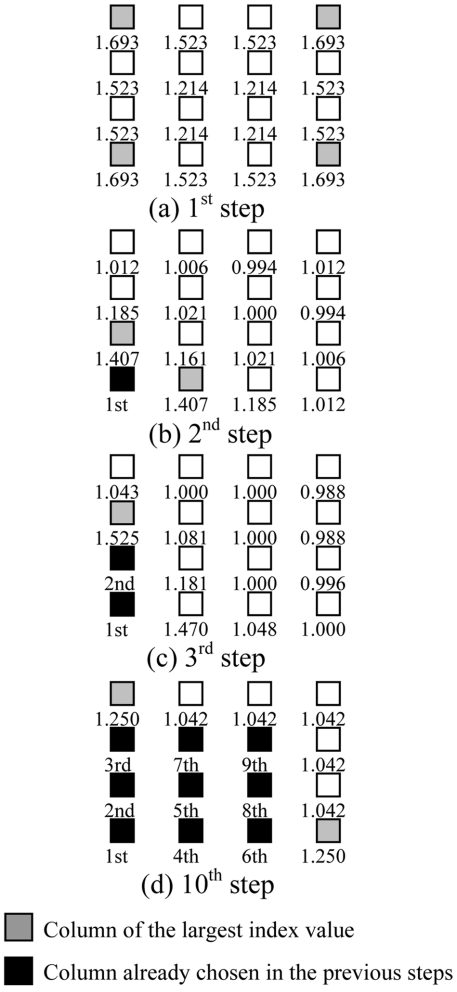

Figure 11. Updated index values and the selection of columns from among those with the largest values (column at the left and lower side is selected prior to the other column if they show same KI values).

the intended demolition direction if the columns are selected from the largest index value. Furthermore, the distribution of the selected columns differs, as shown in Fig. 12, when the columns are selected from the smallest index value. The selected columns tend to distribute the load, stabilizing the structure and preventing instantaneous collapse.

4.2. Blast demolition planning using the integrated values of the key element index

Several blast demolition analyses were performed using selected columns, as described in the previous section. The key element index values of the selected columns are summed and the collapse modes for each case are plotted. Each procedure was performed on models with different floor loads. Fig. 13 shows the distribution of the integrated values of the key element index and the collapse modes of the structure for a simultaneous blast, where nonupdated index values are used. TC in the figures indicates total collapse, PC indicates partial collapse, and NC indicates no collapse. The integrated value indicated by the black circle in Fig. 13(a), for example, is calculated as follows:

$$\begin{aligned} &{}^{0}_{1}KI_1+{}^{0}_{2}KI_5+{}^{0}_{3}KI_9+{}^{0}_{4}KI_2+{}^{0}_{5}KI_6+{}^{0}_{6}KI_3 \\ &=1.693+2.382+3.633+4.284+5.979+7.863 \\ &=25.834 \end{aligned} \tag{12}$$

Here, again, note that the lower right subscript in the key element index indicates the column number, the upper left subscript indicates the step number under consideration in the calculation of the ultimate yield strength ratio, and the lower left subscript indicates the present step number. As shown in the figures, there are certain requirements for the integrated values of the key element index to ensure that the structure is partially or totally demolished. The region of total collapse is large when the columns with the largest index values are successively selected (see Fig. 13(a)), whereas the region is very small when the columns with the smallest index values are selected (see Fig. 13(b)). To accomplish total collapse, neither the integrated index values nor the floor load should be too large because larger values tend to make the structure relatively stable in the collapse process.

Fig. 14 shows the distribution of the integrated values of the key element index and the collapse modes of the structure for sequential blast, where updated index values are used. The integrated value indicated by the black circle in Fig. 14(a), for example, is calculated as follows:

$$\begin{aligned} &{}^{0}_{1}KI_1+{}^{1}_{2}KI_5+{}^{1}_{3}KI_9+{}^{3}_{4}KI_2+{}^{4}_{5}KI_6+{}^{6}_{7}KI_{10} \\ &=1.693+1.407+1.525+1.179+1.315+1.377 \\ &=9.892 \end{aligned} \tag{13}$$

The same tendencies as observed in Fig. 13 can be seen here in the distribution of the index values and the collapse modes. However, the region of total collapse becomes much smaller than in simultaneous blasting because the structure tends to become relatively stable during each blast interval.

It is evident from Figs. 13 and 14 that there are several specific areas of integrated index values that allow for successful demolition, especially when the columns are selected from the largest key element index values. However, the sequential blast of columns from the largest index values causes the whole structure to gradually collapse in sequence, which may, in practical terms, cut the explosive trigger wires and/or make the whole demolition procedure quite unstable. Therefore, the selection of columns with the largest index values may only be used in demolition by simultaneous blasting. In contrast, the selection of columns with the smallest index values may be used to keep the structure stable until the last moment in a demolition by sequential blasting. The structure may be completely demolished by a final blast on a column (or columns) with a large index value, essentially traversing the solid

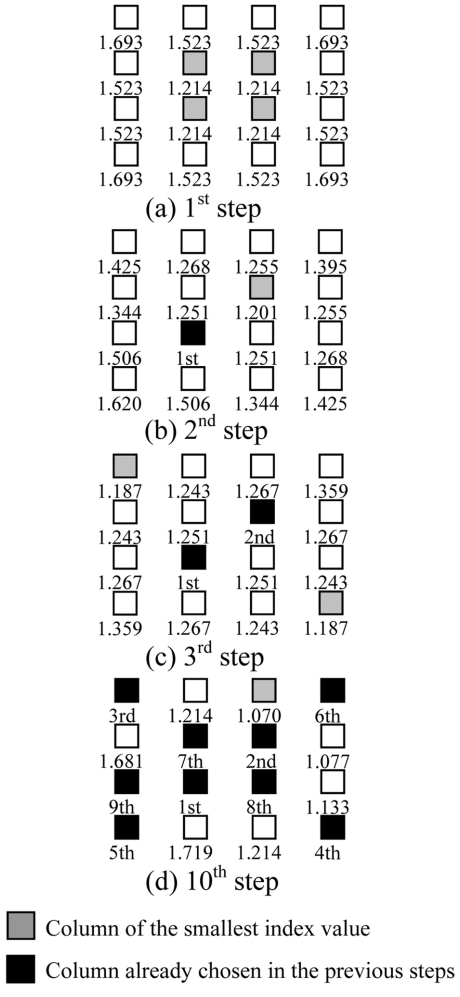

Figure 12. Updated index values and the selection of columns from among those with the smallest values (column at the left and lower side is selected prior to the other columns if they show same KI values).

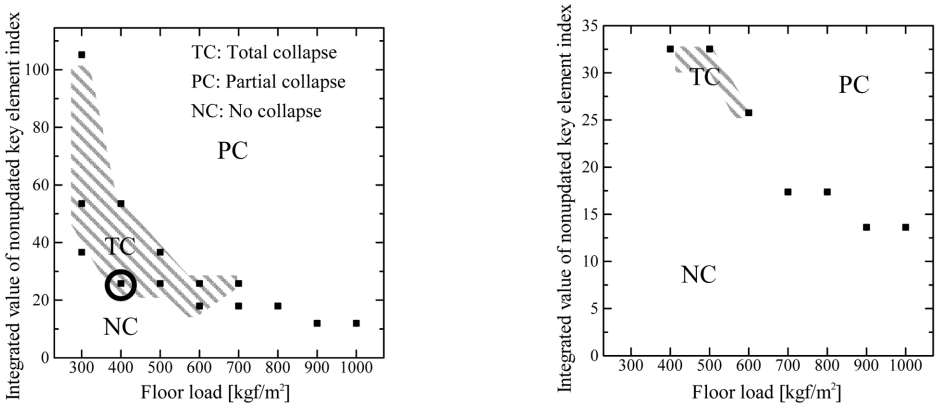

(a) Selecting columns from the largest index value (b) Selecting columns from the smallest index value

Figure 13. Key element index values and collapse behavior of the model (simultaneous blast, nonupdated index value).

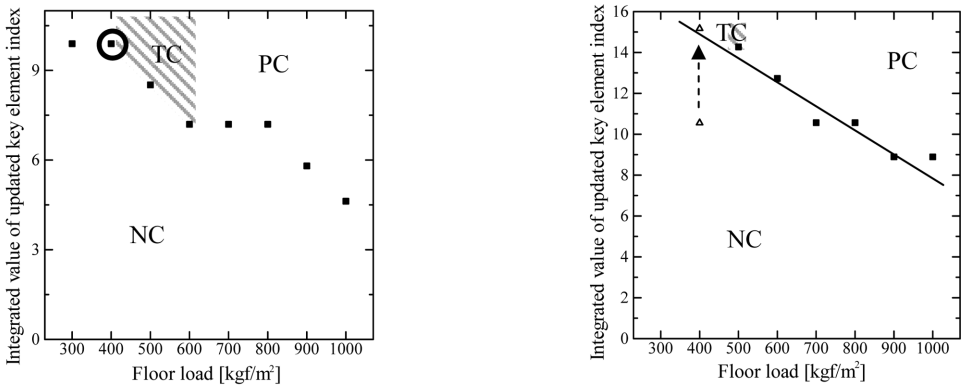

(a) Selecting columns from the largest index value (b) Selecting columns from the smallest index value

Figure 14. Key element index values and collapse behavior of the model (sequential blast, updated index value).

line in Fig. 14(b) in one step.

4.3. Blast demolition analysis of a framed structure using the obtained plan

Two analyses using the plans of blast demolition obtained in the previous section were performed on the model shown in Fig. 10. Each analysis took 50 to 90 minutes on a personal computer (CPU: 2.0 GHz Xeon, 8GB RAM). Fig. 15 shows the demolition mode for the simultaneous blast case, in which the eliminated columns were selected from among those with the largest nonupdated index values. Six columns altogether were selected, in this case, and the integrated value of the key element index was 25.834 as calculated in Eq. (12). Fig. 16 shows the demolition mode for the sequential blast case, in which the columns were selected for elimination from among those with the smallest updated index values. To achieve a total collapse, the columns with the large index values at the final step were selected for the final blast. In this case, nine columns from among those with the smallest index values (with the integrated value of 10.552) were sequentially eliminated over an interval of one second, and then, three columns with the large index values (with the integrated value of 4.614) were simultaneously eliminated at the final blast. Please note that the integrated index value of the initial nine columns does not traverse the solid line in Fig. 14(b), however, the total value including the final three columns, which is 15.166, slightly traverse the line. Although the timings of the collapse initiation and the collapse modes slightly differ in each case, both display a successful demolition pattern, with the structure totally demolished to ground level and towards the intended direction.

5. Conclusions

The numerical code using the ASI-Gauss technique described herein yields highly accurate solutions with small mesh subdivisions and requires little calculation time and a small amount of memory. The shifting of the numerical

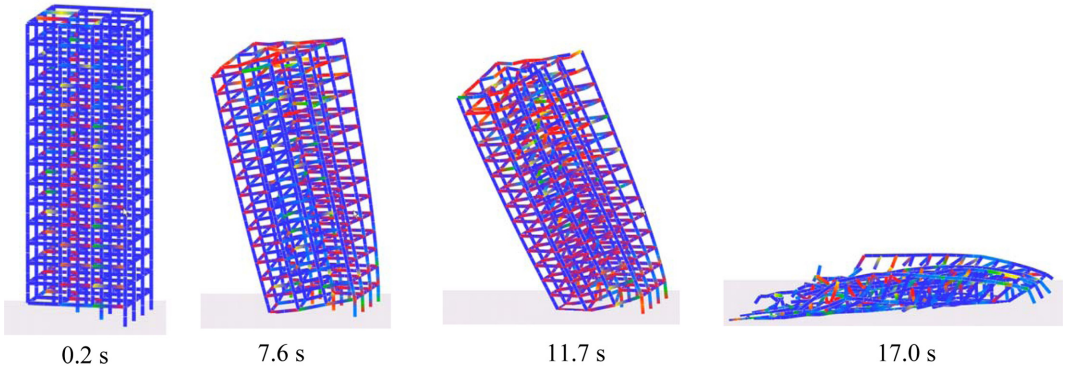

Figure 15. Demolition mode for the simultaneous blast case (six columns selected from the largest nonupdated index value).

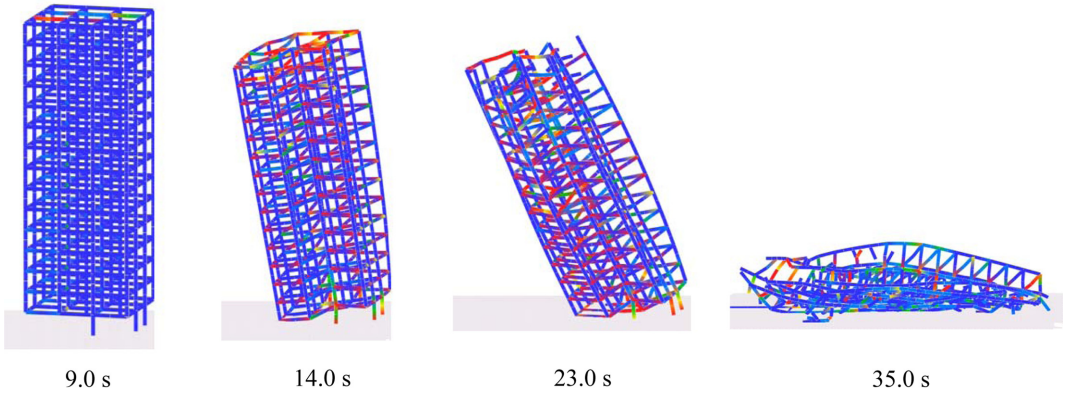

Figure 16. Demolition mode for the sequential blast case (nine columns selected from the smallest updated index values and three columns from the large ones selected for the final blast).

integration points enables the accurate modeling of a fractured section in a member, which is the main reason why the code can be effectively applied to demolition problems. The key element index and its integrated values, as demonstrated in this paper, may be used to quantitatively verify which columns should be eliminated to best achieve a total collapse. The numerical results suggest that for a successful demolition, a group of columns with the largest key element index values should be selected when explosives are ignited in a simultaneous blast, whereas those with the smallest values should be selected when explosives are ignited sequentially, with a final blast set on a column with a large index value. However, further investigation should be undertaken to enable the precise planning of blast intervals and locations required to allow the whole structure to collapse in its own wake, which is very important to lower the risk of damage to neighboring buildings.

6. Acknowledgements

The author would like to express his appreciation for the contributions to the continuous testing and refinement of the code by the former and present graduate students in our laboratory: Kyaw Myo Lynn, Kazunori Shimizu, Kensuke Imanishi, Masashi Eguchi, Zion Sasaki, Tomonobu Omuro, Naoki Katahira, Hitoshi Yokota, Tetsuya Hisanaga, Le Thi Thai Thanh, Yuta Arakaki, Takuya Katsu and Tomoya Ogino.

References

[1] Williams, G. T. (1990). Explosive demolition of tall buildings in inner city areas. *Municipal Engineer*, 7(4), pp. 163~173.

[2] Yarimer, E. (1989). Demolition by Controlled Explosion as a Dynamical Process. *Structures under Shock and Impact*, pp. 411~416.

[3] Kinoshita, M., Hasegawa, A., Matsuoka, S., and Nakagawa, K. (1989). An experimental study on explosive demolition methods of reinforced concrete building. *Proc. of the Japan Society of Civil Engineers*, 403(VI-10), pp. 173~182.

[4] Cundall, P. A. (1971). A Computer Model for simulating Progressive, Large-scale Movement in Blocky Rock Sys-

tem. *Proc. of the International Symposium on Rock Mechanics* II-8, pp. 129~136.
[5] Shi, G. H. and Goodman, R. E. (1984). Discontinuous Deformation Analysis. *Proc. of 25th U.S. Symposium on Rock Mechanics*, pp. 269~277.
[6] Tosaka, N., Kasai, Y., and Honma, T. (1988). Computer Simulation for Felling Patterns of Building. *Demolition Methods and Practice*, pp. 395~403.
[7] Ma, M. Y., Barbeau P., and Penumadu, D. (1995). Evaluation of active thrust on retaining walls using DDA. *Journal of Computing in Civil Engineering*, 1, pp. 820~827.
[8] Itoh, M., Yoshida, N., Utagawa, N., and Kondo, I. (1994). Simulation of Blast Demolition of Reinforced Concrete Buildings. *Proc. of the Third World Congress on Computational Mechanics*, pp. 1152~1153, Chiba, Japan, August 1-5.
[9] Kondo, I., Utagawa, N., Ito, M., and Yoshida, N. (1990). Numerical Method to Simulate Collapse Behavior in Blasting Demolition of Space Framed Structure. *Proc. of the 13th Symposium on Computer Technology of Information, Systems and Applications*, pp. 49~54, in Japanese.
[10] Tagel-Din, H. and Meguro, K. (2000). Nonlinear simulation of RC structures using Applied Element Method. *Structural Engineering / Earthquake Engineering*, 17(2), pp. 137~148.
[11] Lynn, K. M. and Isobe, D. (2007). Finite Element Code for Impact Collapse Problems of Framed Structures, *International Journal for Numerical Methods in Engineering*, 69(12), pp. 2538~2563.
[12] Toi, Y. and Isobe, D. (1993). Adaptively Shifted Integration Technique for Finite Element Collapse Analysis of Framed Structures. *International Journal for Numerical Methods in Engineering*, 36, pp. 2323~2339.
[13] Isobe, D. and Toi, Y. (2000). Analysis of Structurally Discontinuous Reinforced Concrete Building Frames using the ASI Technique. *Computers & Structures*, 76, pp. 471~481.
[14] Toi, Y. (1991). Shifted Integration Technique in One-Dimensional Plastic Collapse Analysis Using Linear and Cubic Finite Elements, *International Journal for Numerical Methods in Engineering*, 31, pp. 1537~1552.
[15] Press, W. H., Teukolsky, S. A., Vetterling, W. T., and Flannery, B. P. (1992). Numerical Recipes in FORTRAN: The Art of Scientific Computing, New York: Cambridge University Press.
[16] Hirashima, T., Hamada, N., Ozaki, F., Ave, T., and Uesugi, H. (2007). Experimental Study on Shear Deformation Behavior of High Strength Bolts at Elevated Temperature. *Journal of Structural and Construction Engineering, AIJ*, 621, pp. 175~180, in Japanese.
[17] Isobe, D., Eguchi, M., Imanishi, K., and Sasaki, Z. (2006). Verification of Blast Demolition Problems Using Numerical and Experimental Approaches. *Proc. of the Joint International Conference on Computing and Decision Making in Civil and Building Engineering (ICCCBE'06)*, pp. 446~455.
[18] Frangopol, D. M. and Curley, J. P. (1987). Effects of Damage and Redundancy on Structural Reliability. *Journal of Structural Engineering, ASCE*, 113(7), pp. 1533~1549.
[19] Ito, T., Ohi, K., and Li, Z. (2005). A Sensitivity Analysis related to Redundancy of Framed Structures Subjected to Vertical Loads. *Journal of Structural and Construction Engineering, AIJ*, 593, pp. 145~151, in Japanese.